Journal of Pharmaceutics & Drug Development
Volume 6 | Issue 1
ISSN: 2348-9782

Research Article Open Access

Solid State Characterization of Consciousness Energy Healing Treated Magnesium Gluconate using PXRD, PSA, DSC and TGA/DTG Analysis

Trivedi D[1] and Jana S[*2]

[1]Trivedi Global Inc., Henderson, USA
[2]Trivedi Science Research Laboratory Pvt. Ltd., Thane, Maharashtra, India

[*]**Corresponding author:** Jana S, Trivedi Science Research Laboratory Pvt. Ltd., Thane, Maharashtra, India, Tel: +91- 022-25811234, E-mail: publication@trivedieffect.com

Citation: Trivedi D, Jana S (2019) Solid State Characterization of Consciousness Energy Healing Treated Magnesium Gluconate using PXRD, PSA, DSC and TGA/DTG Analysis. J Pharma Drug Develop 6(1): 103

Received Date: June 13, 2019 **Accepted Date:** November 19, 2019 **Published Date:** November 21, 2019

Abstract

Magnesium gluconate (Mag-G) is an important nutraceutical and pharmaceutical compound used as a source of magnesium to maintain the overall quality of life as well as for the prevention and treatment of various human diseases. The current study evaluated the influence of the Trivedi Effect® on the physicochemical and thermal properties of Mag-G using sophisticated analytical techniques. Mag-G powder was divided into control and treated parts. The treated part only received the Consciousness Energy Healing Treatment (the Trivedi Effect®) remotely by the well-known Biofield Energy Healer, Dahryn Trivedi. The powder XRD relative peak intensities and crystallite sizes of the characteristic diffraction peaks in the Dahryn's treated Mag-G were significantly altered ranging from -22.13% to 8.37% and -58.36% to 62.54%, respectively compared with the control sample. The average crystallite size of the treated Mag-G was significantly increased by 22.32% compared to the control sample. The particle size values in the treated Mag-G was significantly increased by 3.93% (d_{50}), 37.33% (d_{90}), and 18.71% {D(4,3)} compared with the control sample. Thus, the surface area of the treated Mag-G was decreased by 2.85% compared to the control sample. The heat energy requires to fuse treated Mag-G was increased by 1.52% compared with the control sample. The total weight loss of the treated Mag-G was decreased by 0.92% compared to the control sample. The overall maximum thermal degradation temperature of the treated Mag-G was increased. The thermal stability of the treated Mag-G was improved compared with the control sample. The Consciousness Energy Healing Treatment might have produced a new polymorphic form of Mag-G, which would show better powder flowability and thermal stability compared to the control sample. Thus, Biofield Energy Treated Mag-G would be more advantageous in designing better nutraceutical and pharmaceutical formulations that might provide better therapeutic responses against immunological disorders, cancer, inflammatory diseases, diabetes mellitus, aging, etc.

Keywords: Magnesium Gluconate; Biofield Energy Healing Treatment; The Trivedi Effect®; PXRD; Particle Size; Surface Area; DSC; TGA/DTG

Introduction

Magnesium gluconate (Mag-G) is a classical nutraceutical/pharmaceutical compound used as a source of magnesium. Magnesium is an important essential element for enzymes, DNA, RNA, and protein synthesis in the human body [1-3]. Mag-G is widely used as a supplement in hypomagnesemia and for the prevention and treatment of several diseases, i.e., immunological disorders, inflammatory diseases, allergies, cancer, diabetes mellitus, arrhythmias, asthma, gestational hypertension, septic shock, acute myocardial infarction, eclampsia, preeclampsia, oxidative stress-induced ischemia/reperfusion injury, hearing loss, etc. [4-10]. It has potent antioxidant, oral tocolytic, neuroprotective, and skin-tightening antiaging properties (so used in skin care cosmetics) [11-13]. Mag-G is a physiologically acceptable salt and provides the highest level of magnesium among the other commercially available magnesium salts [4,5,14].

Different religious people recognized a living force that preserves and inhabits in every living organism. This vital force has been scientifically assessed and is now considered the Biofield Energy. The Biofield is an electromagnetic field which exists surrounding the human body, resulting from the continuous movement of the electrically charged particles (charged particle, ions, cells, etc.) in the body and it can release the electromagnetic waves in the form of bio-photons. Such an electromagnetic wave can freely flow between the human and the environment [15]. The expert person has the unique ability to harness energy from the universe and transmit it to any living and nonliving object(s) around the globe via the possible mediation of neutrino [16]. The object or recipient receives Biofield Energy and responds in a useful way [16,17]. The Trivedi Effect®-Biofield Energy Treatment are accepted worldwide for better health and wellness [16]. The National Center of Complementary and Integrative Health has accepted the

Energy Therapy as a Complementary and Alternative Medicine health care approach in addition to yoga, meditation, Tai Chi, Qi Gong, massage, special diets, acupuncture, acupressure, homeopathy, Ayurvedic medicine, traditional Chinese medicines, naturopathy, hypnotherapy, movement therapy, pilates, mindfulness, aromatherapy, Reiki, applied prayer, cranial sacral therapy, etc. [18]. The Trivedi Effect®-Biofield Energy Treatment has gained the importance in several scientific fields includes chemistry, material science, agricultural, microbiology, nutraceuticals, pharmaceuticals, biotechnology, genetics, medical science [19-37] due to its surprising ability to alter the characteristic properties of both the living and non-living objects. The Trivedi Effect® has been reported to have the astounding capability for altering the physicochemical properties of Mag-G after treatment with different healers [34,35]. Hence, the current study was designed to evaluate the impact of the Trivedi Effect® on the physicochemical and thermal properties of Mag-G using various analytical techniques.

Materials and Methods

Chemicals and Reagents

The test sample magnesium (II) gluconate hydrate (98.9%) was procured from Tokyo Chemical Industry Co., Ltd., Japan. However, the light liquid paraffin oil used in the wet method for particle size analysis was procured from Rankem, India.

Consciousness Energy Healing Treatment Strategies

The test compound, Mag-G powder was divided into two parts. One of the test compounds did not receive the Biofield Energy Treatment known as a control Mag-G. But, the control Mag-G was treated with a "sham" healer, who did not have any understanding about the Biofield Energy Treatment. The other part of the test compound received the Consciousness Energy Healing Treatment for 3 minutes remotely by the well-known Biofield Energy Healer, Dahryn Trivedi (USA), and designated as the Biofield Energy Treated Mag-G. Finally, both the samples were stored in similar sealed conditions and characterized using sophisticated analytical techniques.

Characterization

The powder X-ray diffraction (PXRD) analysis of Mag-G powder sample was performed with the help of PANalytical X'Pert3 powder X-ray diffractometer, UK [34,35]. The average size of crystallites was calculated using the Scherrer's formula (1)

$$G = k\lambda/\beta\cos\theta \quad (1)$$

Where, G: crystallite size, λ: radiation wavelength, k: equipment constant, β: full-width half maximum, and θ: Bragg angle [36].

Similarly, the particle size distribution (PSD) analysis was performed with the help of Malvern Mastersizer 3000, UK instrument and Mastersizer V3.50 software using light liquid paraffin oil in the wet method. Further, the differential scanning calorimetry (DSC) analysis of Mag-G was performed with the help of DSC Q200, TA instruments. The thermal gravimetric analysis (TGA) thermograms of Mag-G were obtained with the help of TGA Q50 TA instruments [34,35].

The % change in the treated Mag-G was calculated compared to the control sample using the following equation 2:

$$\%\ \text{Change} = \frac{[\text{Treated} - \text{Control}]}{\text{Control}} \times 100 \quad (2)$$

Results and Discussion

Powder X-ray Diffraction (PXRD) Analysis

The PXRD diffractograms of both the Mag-G samples exhibited sharp and intense peaks (Figure 1). This indicating that both the samples were crystalline in nature. The PXRD data are presented in Table 1.

Entry No.	Bragg angle (°2θ)	Relative Intensity (%)			Crystallite size (G, nm)		
		Control	Treated	% Change	Control	Treated	% Change
1	5.1	93.76	98.68	5.25	34.45	43.07	25.04
2	9.9	36.87	35.11	-4.77	38.38	57.52	49.86
3	10.8	19.27	20.5	6.38	31.42	49.39	57.20
4	13.9	48.96	48.43	-1.08	28.89	38.52	33.36
5	15.9	25.43	24.34	-4.29	34.75	49.65	42.90
6	16.4	16.72	13.02	-22.13	34.77	34.77	-0.01
7	18.1	87.9	78.67	-10.50	29.03	38.72	33.35
8	18.5	72.88	62.66	-14.02	31.70	34.87	10.00

Entry No.	Bragg angle (°2θ)	Relative Intensity (%)			Crystallite size (G, nm)		
		Control	Treated	% Change	Control	Treated	% Change
9	19.1	100.00	100.00	0.00	23.26	24.92	7.14
10	19.5	37.63	35.27	-6.27	34.92	34.91	-0.01
11	19.8	18.51	17.12	-7.51	34.94	34.93	-0.01
12	20.4	28.67	31.07	8.37	34.97	43.72	25.01
13	21.0	23.23	21.19	-8.78	23.33	31.81	36.38
14	22.4	31.65	31.73	0.25	35.09	43.86	25.01
15	23.7	34.97	36.21	3.55	25.11	29.29	16.66
16	24.9	16.18	16.27	0.56	19.57	19.57	-0.03
17	25.5	21.81	21.04	-3.53	27.14	44.11	62.54
18	27.5	25.45	24.65	-3.14	35.43	14.75	-58.36
19	29.0	26.63	27.54	3.42	32.32	44.44	37.52
20	29.4	20.40	18.93	-7.21	29.65	44.48	50.02

Table 1: PXRD data for the control and treated Mag-G

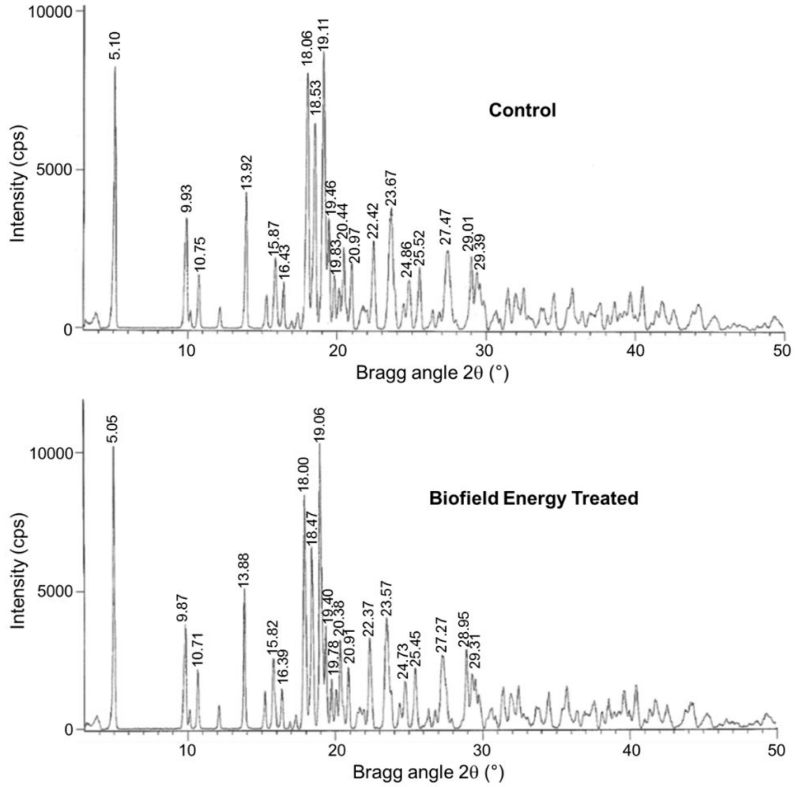

Figure 1: Powder X-ray diffractograms of the control and treated Mag-G

The highest intense peak (100% relative intensity) in the control and Biofield Energy Treated samples were observed at Bragg's angle of 19.1° (Figure 1). The relative peak intensities of the treated Mag-G was significantly altered ranging from -22.13% to 8.37% (Table 1). The crystallite sizes of the Biofield Energy Treated Mag-G was significantly altered ranging from -58.36% to 62.54% compared with the control sample. The average crystallite size of the Biofield Energy Treated Mag-G was significantly increased by 22.32% compared with the control sample.

The alterations in the PXRD patterns such as crystallite size and peak intensities indicated the modification of the crystal morphology, which is the proof of polymorphic transition [37-39]. The crystallite size of the treated Mag-G was significantly altered compared with the control sample, which might produce a new form of Mag-G polymorph. Polymorphic forms of pharmaceuticals have significant effects on drug performance [40,41]. Thus, the Biofield Energy Treatment could be a very useful method for the production of novel crystal polymorph of Mag-G that would offer better drug performance.

Particle Size Analysis (PSA)

The particle size and surface area of the control and Biofield Energy Treated Mag-G were calculated (Table 2). The particle size value at d_{10} in both the sample was very close to each other similar. The particle size values at d_{50}, d_{90}, and D [4,3] in Dahryn's

Biofield Energy Treated Mag-G was significantly increased by 3.93%, 37.33%, and 18.71%, respectively compared with the control sample. Thus, the specific surface area (SSA) of Biofield Energy Treated Mag-G (252.5 m^2/Kg) was decreased by 2.85% with respect to the control sample (259.9 m^2/Kg).

Test Item	d_{10} (µm)	d_{50} (µm)	d_{90} (µm)	D(4, 3) (µm)	Surface area (m^2/Kg)
Control	10.82	26.49	103.48	44.73	259.9
Biofield Energy Treated	10.81	27.53	142.11	53.10	252.5
Percent change (%)	-0.09	3.93	37.33	18.71	-2.85

Table 2: Particle size distribution of the control and treated Mag-G

The particle size and surface area of a pharmaceutical/nutraceutical compound play a vital role in the solubility, dissolution, absorption, and bioavailability in the body [42,43]. The introduction of the Biofield Energy leads to the transform the fine particles into larger particles. The increase the particle size improves the powder flowability, shape, size, and appearance [44,45]. It is assumed that the Trivedi Effect® - Consciousness Energy Healing Treatment might improve the powder flowability, shape, and appearance of Mag-G.

Differential Scanning Calorimetry (DSC) Analysis

The DSC thermograms of the control and Biofield Energy Treated Mag-G exhibited two endothermic peaks (Figure 2). The first small endothermic peak was due to the evaporation of hydrated water molecules from the sample. The second major endothermic peak was because of the melting point of Mag-G. The vaporization temperature and latent heat of vaporization were increased by 2.45% and 6.21%, respectively (Table 3). The melting point of both the Mag-G samples was almost close, but the latent heat of fusion (ΔH_{fusion}) in the Biofield Energy Treated Mag-G was increased by 1.52% compared with the control sample. The increase in particle size increases the melting point and latent heat of fusion [46]. The DSC results were well supported by the particle size data and suggested that the thermal stability of the treated Mag-G was increased compared with the control sample.

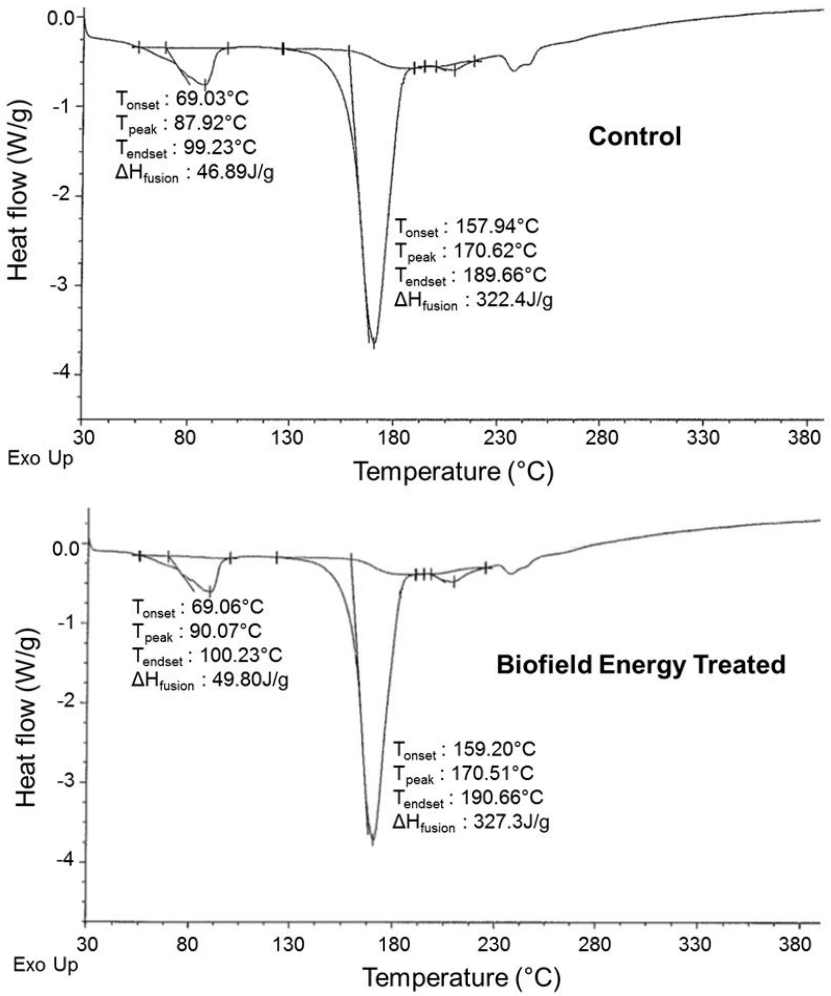

Figure 2: DSC thermograms of the control and treated Mag-G

Peak	Description	Melting Point (oC)	ΔHfusion (J/g)
Peak 1 (Minor)	Control sample	87.92	46.89
	Biofield Treated sample	90.07	49.80
	% Change	2.45	6.21
Peak 2 (Major)	Control sample	170.62	322.40
	Biofield Treated sample	170.51	327.30
	% Change	-0.06	1.52

Table 3: The latent heat of fusion and melting point values of the control and treated Mag-G

Thermal Gravimetric Analysis (TGA) / Differential Thermogravimetric Analysis (DTG)

The TGA study of both the sample of Mag-G exhibited three steps of thermal degradation (Figure 3). The weight loss of the Biofield Energy Treated Mag-G at the 1st and 3rd steps of thermal degradation was significantly decreased by 13.40% and 2.08% compared to the control sample. Whereas, the weight loss of the Biofield Energy Treated Mag-G at the 2nd step of degradation was increased by 2.21% compared to the control sample. The total weight loss of the Biofield Energy Treated Mag-G was decreased by 0.92% compared with the control sample (Table 4).

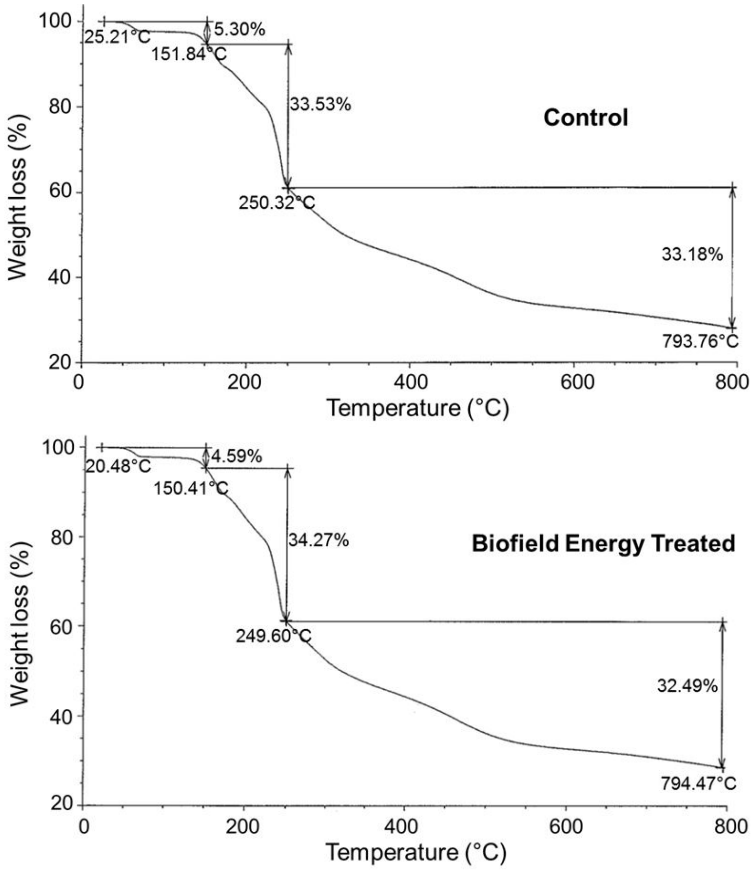

Figure 3: The TGA thermograms of the control and treated Mag-G

Sample	TGA: Weight loss (%)			
	1st step	2nd step	3rd step	Total
Control Sample	5.30	33.53	33.18	72.01
Biofield Energy Treated Sample	4.59	34.27	32.49	71.35
% Change	-13.40	2.21	-2.08	-0.92

Table 4: The TGA thermal degradation steps of the control and treated Mag-G

Similarly, the DTG thermograms of the control and Biofield Energy Treated samples (Figure 4) exhibited four peaks. The maximum thermal degradation temperature (T_{max}) of the Biofield Energy Treated Mag-G was increased by 1.73% (1st), 0.41% (2nd), and 0.33% (3rd) compared to the control sample (Table 5). T_{max} of the 4th peak of the Biofield Energy Treated Mag-G was decreased by 0.22% compared to the control sample (Table 5). Overall, TGA/DTG revealed that the thermal stability of the Dahryn's Biofield Energy Treated Mag-G was significantly improved compared to the control sample.

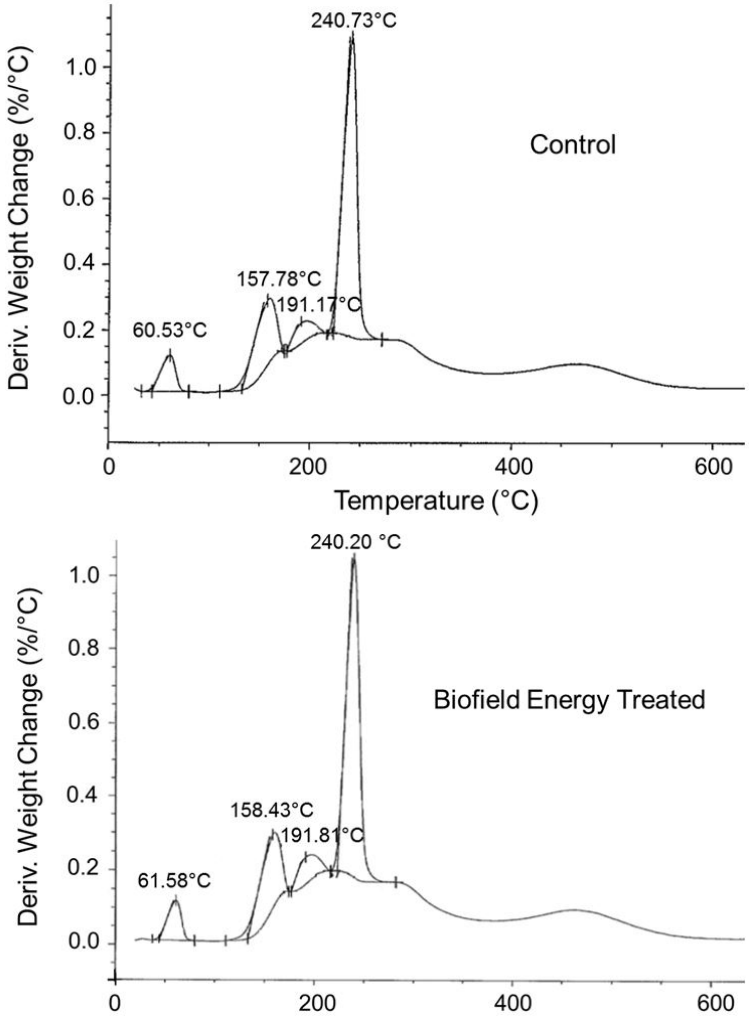

Figure 4: The DTG thermograms of the control and treated Mag-G

Sample	T_{max} (°C)			
	1st step	2nd step	3rd step	4th step
Control	60.53	157.78	191.17	240.73
Biofield Energy Treated	61.58	158.43	191.81	240.2
% Change	1.73	0.41	0.33	-0.22

Table 5: The DTG thermal degradation steps of the control and treated Mag-G

Conclusion

The results indicated that the Trivedi Effect®-Consciousness Energy Healing Treatment revealed a significant effect on the crystallite size, particle size, surface area, and thermal properties of Mag-G. The PXRD relative peak intensities and crystallite sizes of the characteristic diffraction peaks in the Biofield Energy Treated Mag-G were significantly altered ranging from -22.13% to 8.37% and -58.36% to 62.54%, respectively compared with the control sample. The average crystallite size of the Biofield Energy Treated Mag-G was significantly increased by 22.32% compared to the control sample. The particle size values in the treated Mag-G was significantly increased by 3.93% (d_{50}), 37.33% (d_{90}), and 18.71% {D(4,3)} compared to the control sample. Thus, the surface area of the Biofield Energy Treated Mag-G was decreased by 2.85% compared to the control sample. The heat energy requires to fuse the treated Mag-G was increased by 1.52% compared with the control sample. The total weight loss of the treated Mag-G was decreased by 0.92% compared to the control sample. The overall maximum thermal degradation temperature of the treated Mag-G was increased. The thermal stability of the Biofield Energy Treated Mag-G was improved compared with the control sample. The Trivedi Effect®-Consciousness Energy Healing Treatment might have produced a new polymorphic form of Mag-G, which would show better powder flowability and thermal stability compared to the control sample. Thus, Biofield Energy Treated Mag-G would be more advantageous in designing efficacious nutraceutical and pharmaceutical formulations that might provide better therapeutic responses against inflammatory diseases, immunological disorders, cancer, diabetes mellitus, allergies, ischemia/reperfusion injury, septic shock, asthma, eclampsia, arrhythmias, acute myocardial infarction, preeclampsia, hypertension, hearing loss, etc.

Acknowledgement

The authors are grateful to GVK Biosciences Pvt. Ltd., Trivedi Science, Trivedi Global, Inc., and Trivedi Master Wellness for their assistance and support during this work.

References

1. Heaton FW (1990) Role of magnesium in enzyme systems In: metal ions in biological systems, Volume 26: Compendium on magnesium and its role in biology, nutrition and physiology. Marcel Dekker Inc., New York, USA.
2. Frick DN, Banik S, Rypma RS (2007) Role of Divalent Metal Cations in ATP Hydrolysis Catalyzed by the Hepatitis C Virus NS3 Helicase: Magnesium Provides a Bridge for ATP to Fuel Unwinding. J Mol Biol 365: 1017-32.
3. Garfinkel L, Garfinkel D (1985) Magnesium regulation of the glycolytic pathway and the enzymes involved. Magnesium 4: 60-72.
4. Fleming TE, Mansmann Jr HC (1997) Methods and compositions for the prevention and treatment of immunological disorders, inflammatory diseases and infections. United States Patent.
5. Fleming TE, Mansmann Jr HC (1997) Methods and compositions for the prevention and treatment of diabetes mellitus. United States Patent.
6. Guerrera MP, Volpe SL, Mao JJ (2009) Therapeutic uses of magnesium. Am Fam Physician 80: 157-62.
7. Gums JG (2004) Magnesium in cardiovascular and other disorders. Am J Health Syst Pharm 61: 1569-76.
8. Gröber U, Schmidt J, Kisters K (2015) Magnesium in prevention and therapy. Nutrients 7: 8199-226.
9. Weglicki WB (1999) Intravenous magnesium gluconate for treatment of conditions caused by excessive oxidative stress due to free radical distribution. United States Patent.
10. Clague JE, Edwards RH, Jackson MJ (1992) Intravenous magnesium loading in chronic fatigue syndrome. Lancet 340: 124-5.
11. Martin RW, Martin JN Jr, Pryor JA, Gaddy DK, Wiser WL, et al. (1988) Comparison of oral ritodrine and magnesium gluconate for ambulatory tocolysis. Am J Obstet Gynecol 158: 1440-5.
12. Turner RJ, Dasilva KW, O'Connor C, van den Heuvel C, Vink R (2004) Magnesium gluconate offers no more protection than magnesium sulphate following diffuse traumatic brain injury in rats. J Am Coll Nutr 23: 541S-4S.
13. Lee KH, Chung SH, Song JH, Yoon JS, Lee J, et al. (2013) Cosmetic compositions for skin-tightening and method of skin-tightening using the same. United States Patent.
14. Coudray C, Rambeau M, Feillet-Coudray C, Gueux E, Tressol JC, et al. (2005) Study of magnesium bioavailability from ten organic and inorganic Mg salts in Mg-depleted rats using a stable isotope approach. Magnes Res 18: 215-23.
15. Stenger VJ (1999) Bioenergetic fields. Sci Rev Alternative Med 3.
16. Trivedi MK, Mohan TRR (2016) Biofield Energy Signals, Energy Transmission and Neutrinos. Am J Mod Phys 5: 172-6.
17. Rubik B (2002) The biofield hypothesis: Its biophysical basis and role in medicine. J Altern Complement Med 8: 703-17.
18. Koithan M (2009) Introducing complementary and alternative therapies. J Nurse Pract 5: 18-20.
19. Trivedi MK, Branton A, Trivedi D, Nayak G, Saikia G, et al. (2015) chromatographic, spectroscopic, and thermal characterization of biofield energy treated N,N-dimethylformamide. Am J Appl Chem 3: 188-93.
20. Trivedi MK, Branton A, Trivedi D, Nayak G, Saikia G, et al. (2015) Characterization of physico-chemical and spectroscopic properties of biofield energy treated 4-bromoacetophenone. Am J Phys Chem 4: 30-7.
21. Trivedi MK, Nayak G, Patil S, Tallapragada RM, Latiyal O, et al. (2015) Impact of biofield treatment on atomic and structural characteristics of barium titanate powder. Ind Eng Manage 4: 166.
22. Trivedi MK, Tallapragada RM, Branton A, Trivedi D, Nayak G, et al. (2015) Evaluation of physical and structural properties of biofield energy treated barium calcium tungsten oxide. Adv Mater 4: 95-100.
23. Trivedi MK, Branton A, Trivedi D, Nayak G, Mondal SC, et al. (2015) Evaluation of biochemical marker-glutathione and DNA fingerprinting of biofield energy treated Oryza sativa. Am J Biosci 3: 243-8.
24. Trivedi MK, Branton A, Trivedi D, Nayak G, Mondal SC, et al. (2015) Morphological characterization, quality, yield and DNA fingerprinting of biofield energy treated alphonso mango (Mangifera indica L). J Food Nutr Sci 3: 245-50.
25. Trivedi MK, Tallapragada RM, Branton A, Trivedi D, Nayak G, et al. (2015) Evaluation of biofield energy treatment on physical and thermal characteristics of selenium powder. J Food Nutr Sci 3: 223-8.
26. Trivedi MK, Tallapragada RM, Branton A, Trivedi D, Nayak G, et al. (2015) Physicochemical characterization of biofield energy treated calcium carbonate powder. Am J Health Res 3: 368-75.
27. Trivedi MK, Branton A, Trivedi D, Shettigar H, Bairwa K, et al. (2015) Fourier transform infrared and ultraviolet-visible spectroscopic characterization of biofield treated salicylic acid and sparfloxacin. Nat Prod Chem Res 3: 186.
28. Trivedi MK, Branton A, Trivedi D, Nayak G, Bairwa K, et al. (2015) Spectroscopic characterization of disulfiram and nicotinic acid after biofield treatment. J Anal Bioanal Tech 6: 265.
29. Trivedi MK, Patil S, Shettigar H, Bairwa K, Jana S (2015) Evaluation of phenotyping and genotyping characteristic of Shigella sonnei after biofield treatment. J Biotechnol Biomater 5: 196.
30. Trivedi MK, Branton A, Trivedi D, Nayak G, Gangwar M, et al. (2015) Bacterial identification using 16S rDNA gene sequencing and antibiogram analysis on biofield treated Pseudomonas fluorescens. Clin Med 1: 101.
31. Trivedi MK, Branton A, Trivedi D, Nayak G, Gangwar M, et al. (2015) Characterization of phenotype and genotype of biofield treated Enterobacter aerogenes. Transl Med 5: 155.
32. Trivedi MK, Branton A, Trivedi D, Shettigar H, Nayak G, et al. (2015) Phenotyping and genotyping characterization of Proteus vulgaris after biofield treatment. Int J Genet Genomics 3: 66-73.
33. Trivedi MK, Patil S, Shettigar H, Mondal SC, Jana S (2015) The potential impact of biofield treatment on human brain tumor cells: A time-lapse video microscopy. J Integr Oncol 4: 141.

34. Trivedi MK, Branton A, Trivedi D, Nayak G, Plikerd WD, et al. (2017) A systematic study of the biofield energy healing treatment on physicochemical, thermal, structural, and behavioral properties of magnesium gluconate. Int J Bioorg Chem 2: 135-45.

35. Trivedi MK, Branton A, Trivedi D, Nayak G, Wellborn BD, et al. (2017) Characterization of physicochemical, thermal, structural, and behavioral properties of magnesium gluconate after treatment with the Energy of Consciousness. Int J Pharm Chem 3: 1-12.

36. Langford JI, Wilson AJC (1978) Scherrer after sixty years: A survey and some new results in the determination of crystallite size. J Appl Cryst 11: 102-13.

37. Inoue M, Hirasawa I (2013) The relationship between crystal morphology and XRD peak intensity on CaSO4.2H2O. J Crystal Growth 380: 169-75.

38. Raza K, Kumar P, Ratan S, Malik R, Arora S (2014) Polymorphism: The phenomenon affecting the performance of drugs. SOJ Pharm Pharm Sci 1: 10.

39. Brittain HG (2009) Polymorphism in pharmaceutical solids in Drugs and Pharmaceutical Sciences Volume 192, (2nd Edn) Informa Healthcare, Inc., New York, USA.

40. Censi R, Martino PD (2015) Polymorph Impact on the Bioavailability and Stability of Poorly Soluble Drugs. Mol 20: 18759-76.

41. Blagden N, de Matas M, Gavan PT, York P (2007) Crystal engineering of active pharmaceutical ingredients to improve solubility and dissolution rates. Adv Drug Deliv Rev 59: 617-30.

42. Chereson R (2009) Bioavailability, bioequivalence, and drug selection In: Basic pharmacokinetics (1st Edn) Pharmaceutical Press, London, UK.

43. Khadka P, Ro J, Kim H, Kim I, Kim JT, et al. (2014) Pharmaceutical particle technologies: An approach to improve drug solubility, dissolution and bioavailability. Asian J Pharm Sci 9: 304-16.

44. Kale VV, Gadekar S, Ittadwar AM (2011) Particle size enlargement: Making and understanding of the behavior of powder (particle) system. Syst Rev Pharm 2: 79.

45. Podczeck F, Mia Y (1996) The influence of particle size and shape on the angle of internal friction and the flow factor of unlubricated and lubricated powders. Int J Pharm 144: 187-94.

46. Zhang M, Efremov MY, Schiettekatte F, Olson EA, Kwan AT, et al. (2000) Size-dependent melting point depression of nanostructures: Nanocalorimetric measurements. Phys Rev B 62: 10548.